

# A Unified Approach to (*E*)- and (*Z*)-Olefins Enabled by Low-Valent Tungsten Catalysis

Tanner C. Jenkins, Camille Z. Rubel, Hang Chi Ho, Raul Martin-Montero, Keary M. Engle\*

Department of Chemistry, The Scripps Research Institute, 10550 North Torrey Pines Road, La Jolla, California 92037, United States

**ABSTRACT:** Achieving regio- and stereoselective formation of products from simple chemical building blocks is one of the most important roles of catalysis in organic synthesis. Repositioning an alkene functional group through catalytic alkene isomerization represents a powerful synthetic strategy for preparing valuable alkene products from comparatively simple chemical feedstocks. The utility of this approach, however, hinges on the ability to control the positional and stereoisomerism to access a single product among numerous potential isomeric byproducts. Here, a positionally selective alkene isomerization in which modulation of the ligand environment of the homogeneous tungsten catalyst grants access to either the (*E*)- or (*Z*)-stereoisomer is described. Compared to previously reported alkene isomerization methods, this reaction offers exquisite chemo- and regioselectivity from a simple, commercially available precatalyst and ligand. Preliminary mechanistic studies suggest that tungsten's ability to adopt 7-coordinate geometry is crucial for stereoselectivity and that substrate directivity prevents over-isomerization to the conjugated alkene, as is commonly observed with other catalysts. These features allow for exclusive formation of  $\beta,\gamma$ -unsaturated carbonyl compounds that are otherwise difficult to prepare.

## Introduction

Alkenes are common functional groups in numerous natural products,<sup>1-5</sup> fragrances,<sup>6</sup> and materials, and they serve as versatile intermediates in organic synthesis.<sup>7-11</sup> Accessing alkenes as single positional and *E/Z*-stereoisomers is essential, given that their chemical, physical, or biological properties stem from these structural features, as does their synthetic utility. Due to the importance of these motifs, a chemical method that can accomplish the controlled formation of either *E*- or *Z*-alkenes from a single starting material would be highly desirable.

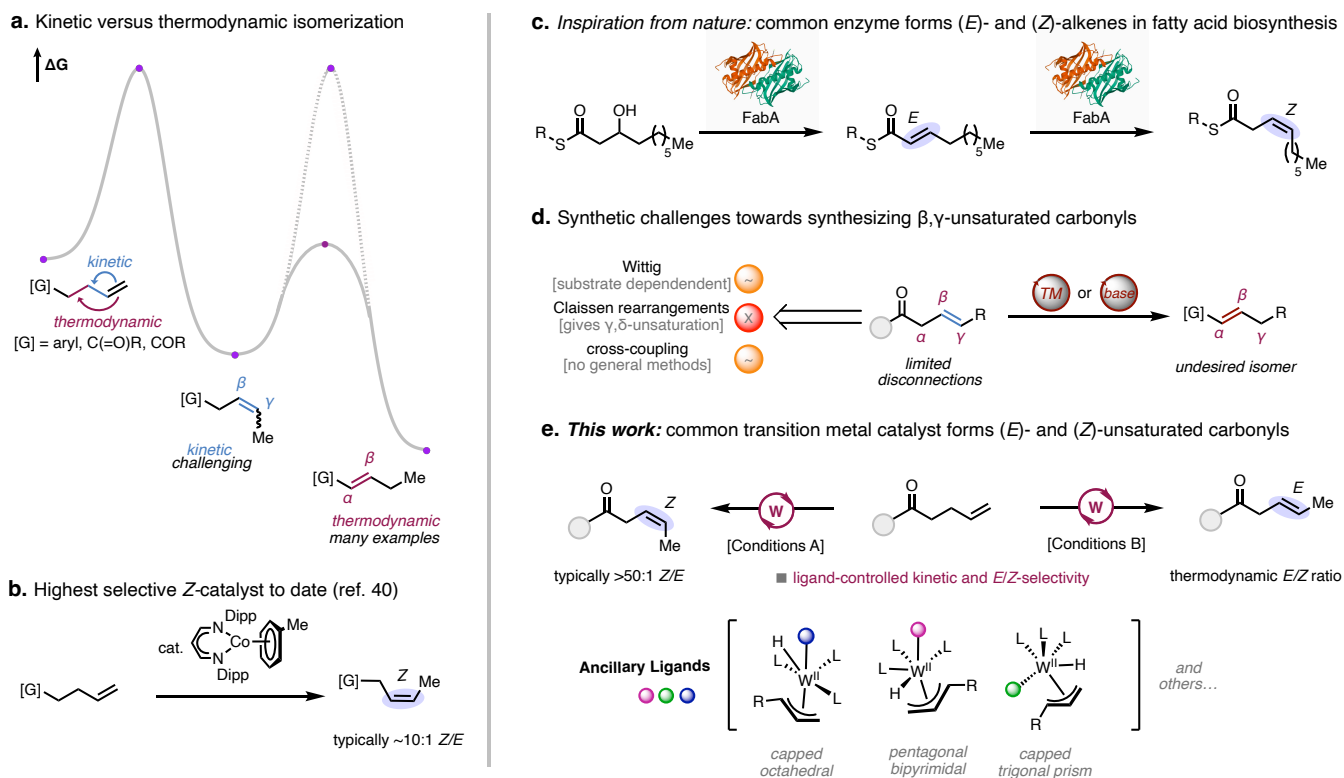


**Figure 1:** (a) Possible stereo- and regioisomeric outcomes of alkene isomerization. This model free energy diagram depicts a hypothetical isomerization from terminal, to (*Z*) 2-alkene (kinetic product), to the conjugated alkene

(thermodynamic product). **(b)** Holland's cobalt catalyst that exhibits high *Z*-selectivity.<sup>40</sup> **(c)** Fatty acid synthesis involving formation of different *E*- and *Z*-alkenes from a single enzyme FabA. Protein image taken from rcsb.org; PDB code: 7BIS **(d)** Classic disconnections towards alkenes synthesis and the pitfalls of using them to synthesize  $\beta,\gamma$ -unsaturated carbonyls. **(e)** This approach: ligand-controlled formation of *E* or *Z* alkenes using a low-valent tungsten catalyst.

Catalytic alkene transposition represents a promising and atom-economical strategy for alkene synthesis<sup>7-9,12-17</sup> but necessitates multiple levels of selectivity control to access the product as a single positional and stereoisomer.<sup>18-28</sup>

In particular, most catalytic alkene isomerizations are thermodynamically controlled and bring about migration of the alkene into conjugation with adjacent functional groups (Figure 1a).<sup>29-39</sup> Selecting for a single kinetic internal alkene isomer remains difficult in general,<sup>40-46</sup> particularly when the newly formed products possess C(allylic)–H bonds that are activated by an adjacent functional group (e.g., carbonyl). Such non-conjugated internal alkenes are valuable synthetic targets as there are fewer associated retrosynthetic disconnections compared to their conjugated counterparts (Figure 1d). In these cases, classical methods such as Wittig olefination,<sup>47</sup> Mizoroki–Heck reaction,<sup>48-49</sup> alkenyl Suzuki–Miyaura coupling,<sup>50-51</sup> and alkyne semi-hydrogenation<sup>52-55</sup> can readily promote isomerization of the initially formed alkene product to the thermodynamically favored conjugated alkene due to the presence of catalytic base or transition metal, such as palladium.

Over the past 60 years, a variety of kinetic alkene isomerization catalysts have emerged, mostly using precious metals (e.g., Ru, Ir, and Pd). In rare instances, non-precious metals can be utilized, including Holland's Co catalyst providing the challenging *Z*-isomer with high (>10:1) selectivities (Figure 1b),<sup>40,44</sup> and Doberiner's Mo catalyst furnishing moderate (~3:1) selectivity.<sup>41</sup> However, these catalysts and most others require multi-step synthesis under rigorously inert conditions, thus limiting their accessibility and appeal to the synthetic community. The Ni-catalyzed methodology of Hilt offers variable *Z*-selectivity (ranging from 3:1 to >99:1) and requires cryogenic temperatures, which introduces substrate insolubility issues and makes it difficult to scale up.<sup>43</sup> *E*-Selective transposition catalysts based on precious metals that offer high *E*-selectivity do so at the cost of varying levels of "over-isomerization" to give a mixture of multiple alkene isomers.<sup>19, 21-23, 25-26, 28</sup> We sought to address this limitation by developing a method exhibiting high functional group tolerance, minimal over-isomerization of the desired kinetic product, and operational simplicity using a simple (ideally commercially available) non-precious metal catalyst and ligand.

In nature, simple building blocks can be converted into either *E*- or *Z*-alkene isomers by enzymatic machinery; for example, in the type II fatty acid synthase system of *Escherichia coli*., a single enzyme FabA converts  $\beta$ -hydroxyl esters into an *E*-alkene and subsequently its deconjugated *Z*-isomers (Figure 1c).<sup>56-58</sup> Taking inspiration from this biosynthetic approach, here we demonstrate a method in which readily accessible  $\gamma,\delta$ -unsaturated carboxylic acid derivatives are isomerized into  $\beta,\gamma$ -unsaturated products, granting access to a single positional isomer with control of *E/Z*-stereochemistry.

Based on our recent findings<sup>59-60</sup> on the tungsten-catalyzed tandem alkene isomerization/functionalization using the W(0)/(II) redox couple, we envisioned that the ability of 7-coordinate W(II) to readily adopt different molecular geometries and ligand configurations could be exploited to control the stereochemical outcome of the products. Specifically, we sought to develop an alkene isomerization whereby ligand induced modulation of the key 7-coordinate W(II) intermediate would allow for selection for either the *E*- or *Z*-product (Figure 1e). In addition, we believed high positional selectivity for the kinetic (i.e. non-conjugated) product could be achieved using a W(0) catalyst, even with substrates that can readily form the thermodynamically favored conjugated alkene.

## Reaction optimization

We began this study by evaluating the commercially available W(MeCN)<sub>3</sub>(CO)<sub>3</sub> precatalyst and commercial ligands for their ability to perform kinetic isomerization of  $\gamma,\delta$ -unsaturated amide **1a**. This substrate was selected based on the established ability of the amide group to coordinate to the tungsten catalyst<sup>60</sup> and because it offered a challenging test case in selectivity control in which over-

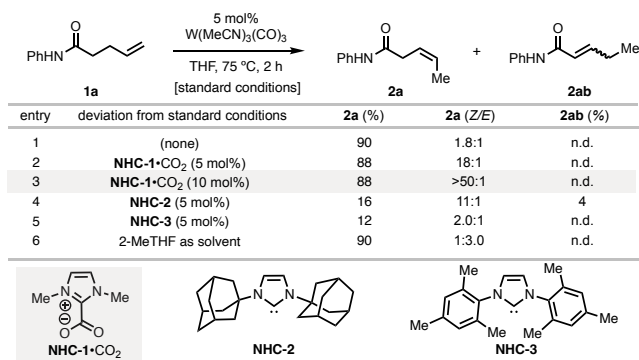


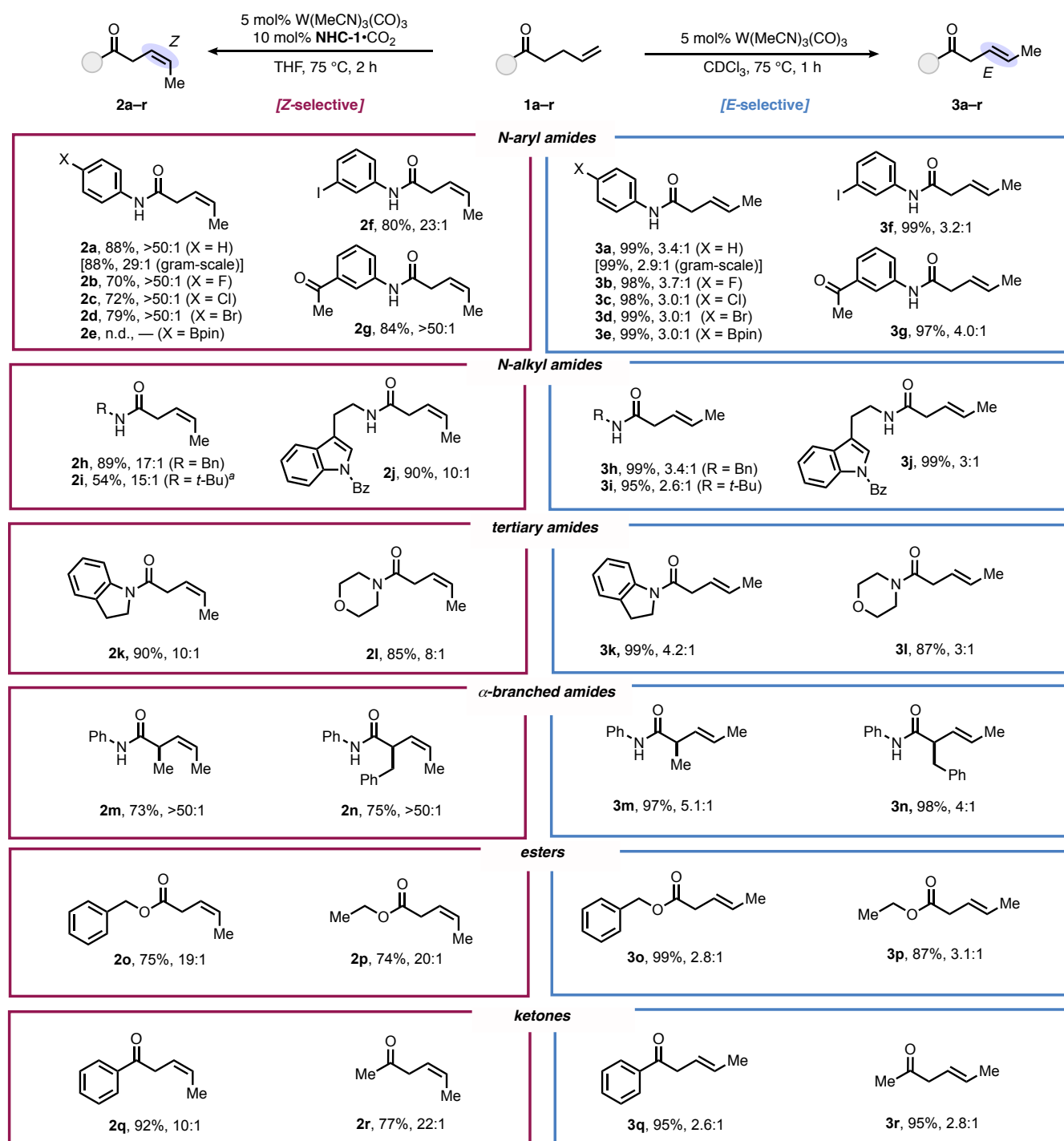
**Table 1:** Optimization of the reaction conditions for *Z*-selectivity.<sup>a</sup> *E/Z* ratio and product distributions determined <sup>1</sup>H NMR (n.d. = not detected). Remaining material was unreacted **1a** in all cases.

isomerization would need to be avoided. Early observations showed that using THF as the solvent provided the *Z*-isomer in 1.8:1 selectivity, suggesting that THF may serve as a ligand (Table 1, entry 1). In support of this hypothesis, the use of less-coordinating 2-MeTHF gave the *E*-isomer as the major product (entry 6). With this hypothesis in mind, we next turned to *N*-heterocyclic carbene (NHC) ligands, which have a similar 5-membered ring structure as THF, from which we identified **NHC-1** as the optimal ligand giving 18:1 *Z*-selectivity (entry 3). Excess ligand (entry 4) was used to ensure that no background isomerization occurred from non-ligated tungsten species, resulting in >50:1 *Z*-selectivity. Increasing the steric bulk of the nitrogen substituents decreased the *Z*-selectivity and yield (entries 4–5). Starting from the carboxylate “pre-NHC” allows for base-free activation to form the free carbene and thus circumvents base-mediated over-isomerization observed when using KO*t*-Bu and the imidazolium salt (See Table S3).<sup>61</sup> *E*-Selective conditions were also identified using a non-coordinating solvent, CDCl<sub>3</sub>, without added ligand (See Table S1 for optimization). The *E/Z* ratios obtained under these conditions of approximately 3:1–4:1 are in line with the expected thermodynamic ratios based on an energy difference between the (*E*)- and (*Z*)-isomers of ~0.4 kcal/mol at 23 °C.<sup>62</sup> Although the selectivity is seemingly modest, our results are on par with even the best catalysts for this type of alkene transposition.<sup>40, 42</sup> In general, the inability to gain higher *E*-selectivity can be explained if the isomerization is kinetically selective in terms of alkene position but thermodynamically controlled in terms of alkene stereochemistry. While there are specific substrates which can overcome the thermodynamic control of *E*-stereochemistry, this remains an unmet challenge.

### Substrate scope

We next investigated the generality of the *Z*-selective isomerization method with various  $\gamma,\delta$ -unsaturated carboxamides. A range of secondary *N*-aryl amides with functional groups at the *para* position proceeded in high yield with >50:1 *Z*-selectivity (**2a–d**). Potentially reactive functional groups were tolerated, including an iodo substituent (**2f**), providing a handle for further derivatization of these valuable products via cross-coupling (vide infra). An unhindered ketone, which could be readily reduced by the propagating M–H species generated in other isomerization methods also gave the product in high yield and selectivity (**2g**). Additionally, secondary *N*-alkyl alkenyl amides were effective substrates, offering very good *Z*-selectivity (**2h–2j**, 10–17:1) even with the bulky *tert*-butyl group (**2i**). Tertiary amides with pharmaceutically relevant heterocycles provided high yields with slightly diminished selectivity (**2k** and **2l**, 8–10:1). In general, alkyl substituents on the amide decreased *Z*-selectivity, which could potentially be due to the stronger coordination of the more Lewis basic amide carbonyl to tungsten enabling the catalyst to reengage the product in secondary *Z*-to-*E* isomerization. *A*-Branched substrates **2m** and **2n** gave >50:1 *Z*-selectivity, despite the increased allylic strain. In addition to amides, esters (**2o** and **2p**) and ketones (**2q** and **2r**) also performed well, providing excellent selectivity and high yields. That the method is compatible with these substrates supports a mechanism involving coordination of tungsten through the carbonyl and not the nitrogen of the amide. We then assessed the substrate scope with the optimized *E*-selective conditions and found the protocol to give high to quantitative yields when using the same alkenyl amides previously assessed with the *Z*-selective conditions. The reaction was scalable, providing more than 1 gram of product without change in yield and only a modest erosion of *E/Z* selectivity under both conditions. Notably, substrate **3e**, which possesses an aryl boronate motif, performed well under these conditions, despite giving no reaction when tested with the *Z*-selective conditions. For all substrates, the *E/Z* selectivity appears to reflect the thermodynamic ratio for internal 1,2-dialkyl-substituted alkenes.<sup>62</sup> These findings are in line with previous one-position isomerizations with non-precious-metal catalysts, with improved *E*-selectivity observed in only rare cases typically involving precious metal catalysts.<sup>18–28</sup> The higher *E*-selectivity for  $\alpha$ -branched substrates **3m** and **3n** (4–5.1:1) can be explained by increased allylic strain.

**Table 2:** Substrate scope for *Z*- (left) and *E*- (right) selective alkene transposition of  $\gamma,\delta$ -unsaturated carbonyl compounds.



<sup>a</sup> Reaction performed at room temperature.

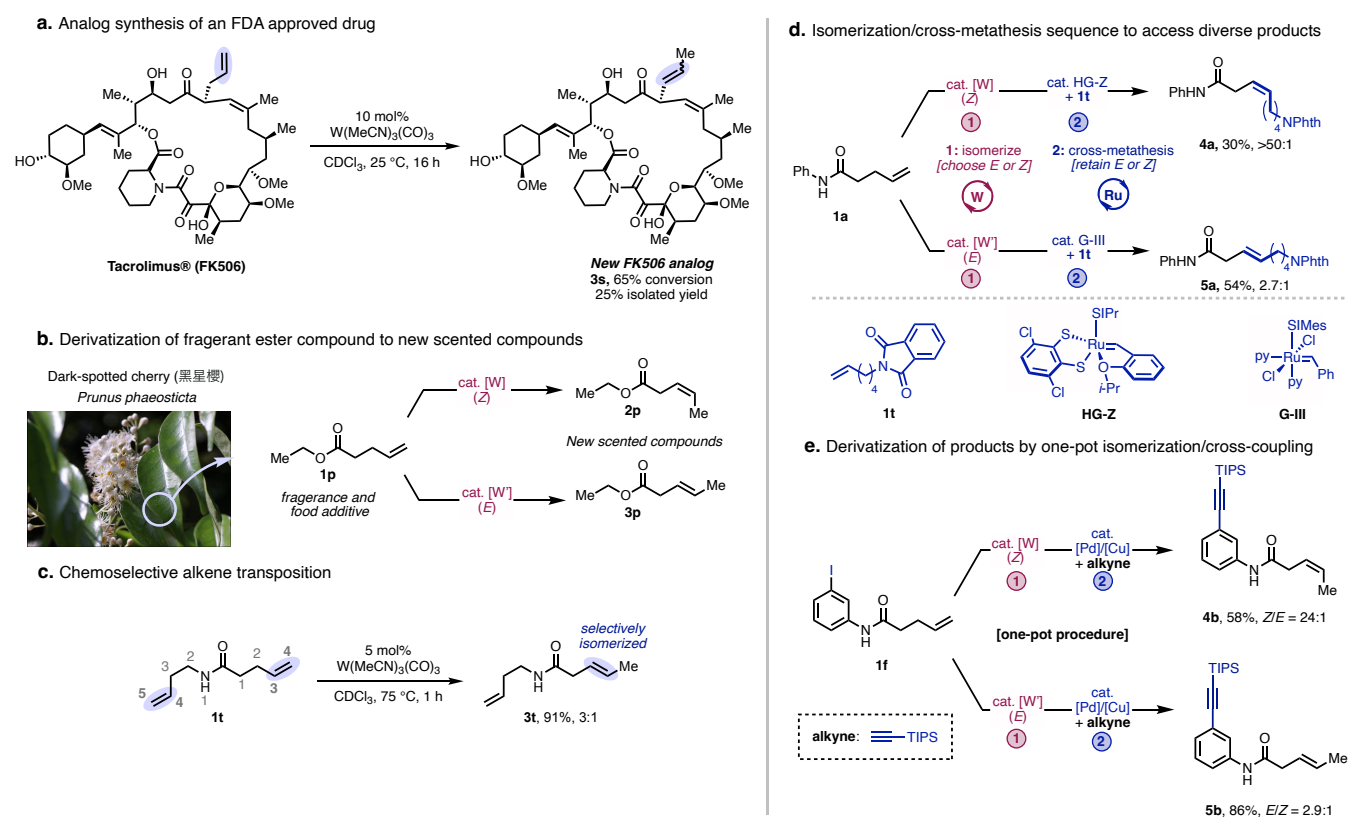
### Synthetic applications and product diversification

To demonstrate applications of this method in the context of a challenging drug discovery problem, we chose to modify the FDA approved drug FK506 (Tacrolimus®) (Scheme 1a). Interestingly, synthesis of this analog (**3s**) has not been previously reported, and therefore we anticipate this new analog to garner much interest from medicinal chemistry. Specifically, this portion of the molecule binds calcineurin,<sup>63</sup> and small modifications to this section of the molecule have been shown to have enhanced effects such as with the analog FK520.<sup>64</sup> To further demonstrate applications to the food and fragrance industry, we were able to derivatize the natural product **1p** which is derived from the dark-spotted cherry (*Prunus phaeosticta*) and has a sweet ethereal scent (Scheme 1b).<sup>65</sup> By affecting olefin

isomerization, we were able to synthesize two new scented compounds (**2p** and **3p**) via the *Z*- and *E*-selective protocols respectively.

We envisioned that the substrate-directed nature of this isomerization system and the exquisite chemoselectivity of the tungsten(0) catalyst could be leveraged to achieve selective isomerizations that are inaccessible via alternative approaches. To this end, exposing diene **1t** to the standard *E*-selective conditions brought about exclusive isomerization of the proximal alkene on the carbonyl side of the amide, demonstrating differentiation based solely on the presence of an intervening NH group (Scheme 1c).

By parlaying the stereoselective isomerization into a subsequent cross-metathesis we devised a two-step sequence to access a variety of internal  $\beta,\gamma$ -unsaturated amides that are otherwise difficult to prepare in a stereoselective fashion (Scheme 1d). The utility of this approach stems from the widespread availability of terminal alkenes and  $\gamma,\delta$ -unsaturated carboxylic acid derivatives, the latter of which can be conveniently prepared via Johnson–Claisen rearrangement and other established methods. Evaluation of several ruthenium metathesis catalysts revealed that a stereoretentive dithiolate catalyst<sup>66</sup> could convert the *Z*-alkenyl amide into the desired final product with >50:1 selectivity, showing no *E/Z*-erosion compared to the first step. Moreover, Grubbs third-generation bis-pyridine catalyst<sup>67</sup> could be used to furnish the *E*-enriched internal alkene product in the thermodynamic 2.7:1 product ratio.



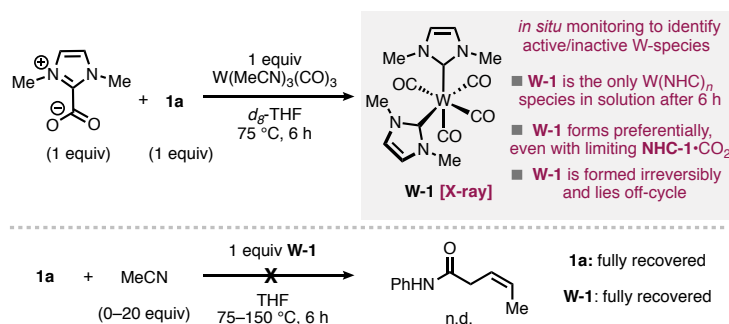
**Scheme 1:** (a) Late-stage modification of FDA approved to form a new synthetic analog **3s**. (b) Derivatization of known fragrant compound **1p**, which is extracted from the leaves of the dark-spotted cherry shown in the picture. (c) Highly chemoselective isomerization of only one alkene of a diene based on substrate directivity. (d) Application of sequential stereoselective alkene isomerization/stereoretentive cross-metathesis. Reported yields and selectivity's correspond to the second step. (e) Application of a one-pot alkene isomerization followed by Sonogashira cross-coupling reaction to diversify the aryl iodide substrates **2f** and **3f**.

To demonstrate the utility of this procedure, derivatization of latent functional handles was performed after alkene isomerization. Crude products **2f** and **3f** smoothly underwent a telescoped Pd/Cu-catalyzed Sonogashira coupling, maintaining the alkene stereochemistry established during isomerization without removal of the spent tungsten catalysts (Scheme 1e).

#### Mechanistic studies

To determine the origins of stereoselectivity, we sought to understand catalyst speciation and the ligand environment around the metal during catalytic turnover. Regarding the *Z*-selective conditions, we reasoned that catalyst deactivation was likely at play, as extending the reaction time from 2 to 48 h did not increase conversion

of unreacted starting material to product beyond 88% and did not change the final *E/Z*-selectivity. *In situ* monitoring of a stoichiometric reaction by NMR revealed the emergence of multiple  $^{13}\text{C}$  peaks from  $\text{W}(\text{NHC-1})_n$  species after 1 h. At extended reaction times, these converged to a single  $\text{W}(\text{NHC-1})_2$  species, **W-1** (Scheme 2). Complex **W-1** was isolated, and its structure confirmed by single-crystal X-ray crystallography. Resubjecting **W-1** to the standard reaction conditions resulted in no isomerization of the alkene, with complete recovery of both starting material and catalyst, even when the temperature was increased to 150 °C. This result establishes that **W-1** is not catalytically competent and is thus off-cycle and formed irreversibly. The formation of bis-NHC tetracarbonyl species **W-1** appears to be favored irrespective of the amount of NHC added (0.5–4 equiv) and likely arises from CO ligand disproportionation, as previously observed by our lab<sup>59</sup> and Figueroa<sup>68</sup> in the synthesis of low-valent W complexes. A priori, we envisioned two potential mechanisms for alkene transposition; (1) a metal–hydride insertion-elimination pathway, and (2) a  $\text{W}(\pi\text{-allyl})(\text{H})$  pathway.<sup>69</sup> Radical based pathways can be ruled out as this would require tungsten have unpaired electrons, which is energetically infeasible with the strong ligand field of low-valent  $\text{W}\text{-CO}$  complexes.<sup>70-71</sup> A concise set of deuterium-labeling experiments were performed to gain insight into the mechanism of isomerization. An initial experiment with N–D labeled secondary amide **1a-d<sub>1</sub>** provided no deuterium incorporation under *E*- or *Z*-selective conditions, ruling out N–H/D oxidative addition as a mechanism for generating a  $\text{W}(\text{II})(\text{H}/\text{D})$  species (Scheme 3b top). This result in combination with there being no other clear hydride sources from the substrate, ligands, or the solvent strongly disfavors pathway 1. On the other hand, D-labeling of the allylic C–H position (**1a-d<sub>2</sub>**) resulted in the expected 1,3-H/D shift, supporting the formation of a  $\text{W}(\text{II})(\pi\text{-allyl})(\text{H})$  through allylic C–H/D oxidative addition (Scheme 3b, middle). Interestingly, whereas the *Z*-selective conditions had high fidelity of intramolecular deuterium retention, the *E*-selective conditions resulted in significant intermolecular D-scrambling. Further evidence for an intermolecular D-exchange was observed in a crossover experiment between **1a-d<sub>2</sub>** and tertiary amide **1k** (Scheme 3b, bottom). While intermolecular H/D scrambling is typically an artifact of pathway 1, Ogoshi has shown that bis alkene complexes  $\text{M}(\text{alkene})_2\text{L}_n$  can also undergo intermolecular H/D scrambling through pathway 2 type mechanisms albeit as a minor side pathway, with similar D-labeling experimental results as this study.<sup>72</sup> Although no D-labeling was done, Szymańska-Buzar has also shown that  $\text{W}(\text{alkene})_2\text{CO}_4$  complexes are known to isomerize the alkene through 1,3-H shift mechanisms, suggesting bis alkene intermediates may be catalytically competent and involved in minor side pathways.<sup>70</sup>

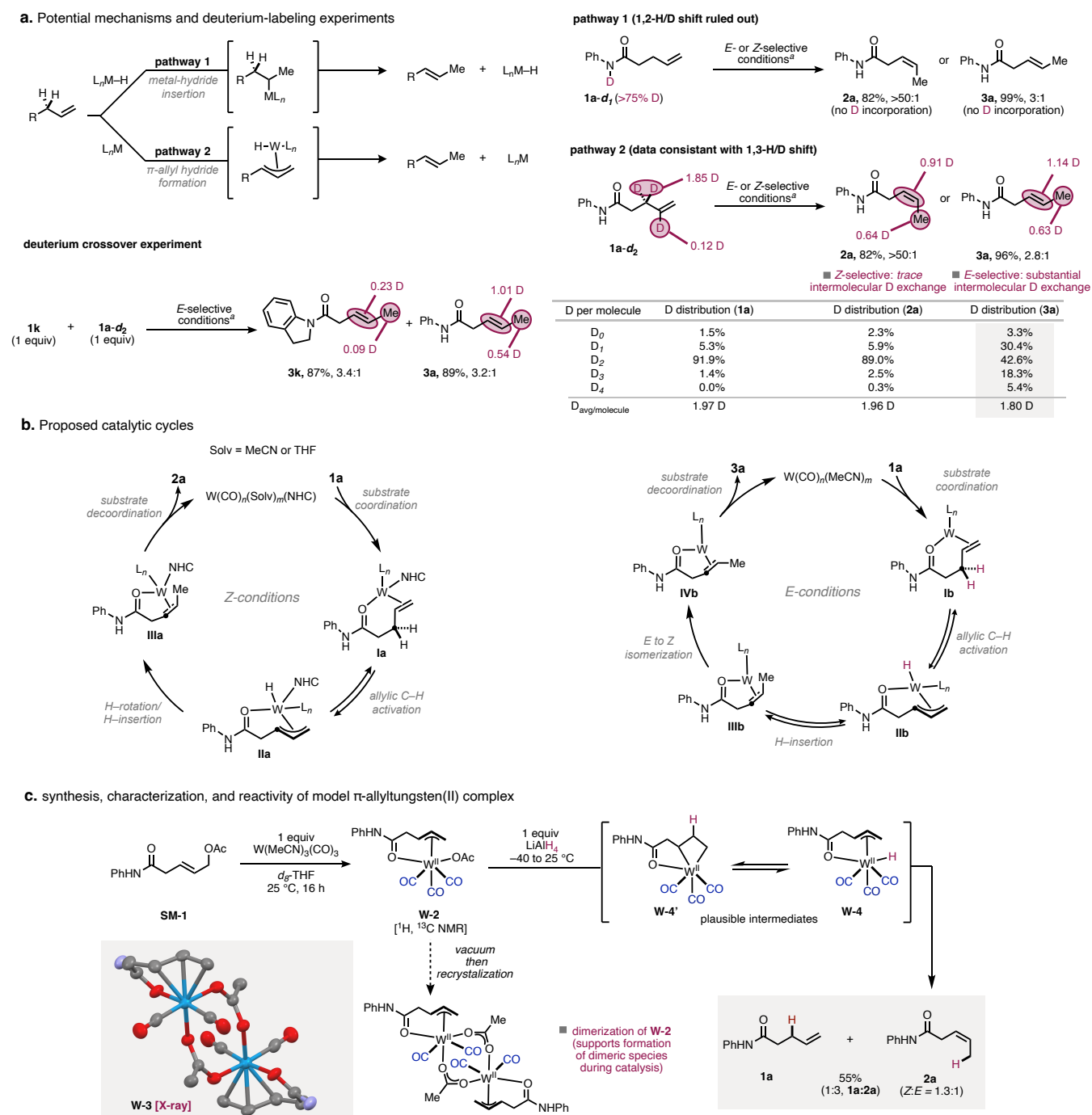


**Scheme 2.** Determination of catalyst speciation and characterization of off-cycle species that results in catalyst death.

We then sought to identify catalytically active or off-cycle species by *in situ* NMR. However only free alkene **1a** and **3a** could be observed over a range of temperatures (4–75 °C) with no substrate coordinated species easily identified. For this reason, we sought to target stable progenitor complexes through independent synthesis that could be converted into a reactive  $\text{W}(\text{II})(\pi\text{-allyl})(\text{H})$  species to shed light on the underlying coordination chemistry and reactivity. To this end, treatment of amide-containing allyl acetate **SM-1** with  $\text{W}(\text{MeCN})_3(\text{CO})_3$  in THF at room temperature yielded chelated  $\text{W}(\text{II})(\pi\text{-allyl})(\text{acetate})$  oxidative addition adduct **W-2** (Scheme 3a). Concentration of the solution and recrystallization afforded the dimeric species **W-3**. This structure provides further evidence for coordination of tungsten through the carbonyl of the amide and explains why sterically bulky groups on nitrogen have minimal effect on the reaction. In each of the monomeric units of **W-3**, the metal center is approximately capped octahedral geometry, with the CO ligands oriented in the most thermodynamically favored configuration facing the “open face” of the  $\pi$ -allyl fragment.<sup>73-74</sup> While at present it is difficult to determine the exact geometries and 3D ligand configuration responsible for *E* versus *Z*-selectivity, it appears that the CO ligands and the amide carbonyl play a critical role in controlling the geometry of the  $\text{W}(\text{II})$  intermediate and preventing over-isomerization into conjugation.

Reaction between **W-2** and  $\text{LiAlH}_4$  at –40 °C furnished a mixture of organic products, with the major products being *E/Z*- $\beta,\gamma$ -unsaturated amides **2a** and **3a** and the minor product being  $\gamma,\delta$ -unsaturated amide **1a**. Mechanistically,

this is consistent with a sequence involving transmetalation to furnish reactive  $W(II)(\pi\text{-allyl})(H)$  intermediate **W-4** (which could further react via reversible hydride insertion to form metallocyclobutane **W-4'**).<sup>75</sup> C(allyl)-H reductive elimination from **W-4** forms **1a**, **2a**, or **3a**. Interestingly, the *Z/E* ratio (**2a:3a** = 1.3:1) is approximately equal to the ratio obtained when only THF is used as solvent without additional ligand (1.8:1, see Table 1, entry 1), which corroborates the validity of this model system. Formation of  $\gamma,\delta$ -unsaturated amide **1a** (the starting material in the catalytic kinetic isomerization) suggests that the initial C(allyl)-H activation step may be reversible. Attempts to exchange a CO ligand for NHC-1 or exchange the acetate for another X-type ligand were unsuccessful, resulting in decomposition of **W-2** and formation of intractable product mixtures that could not be separated or assigned by NMR. Although these experiments were not performed under the exact conditions of the catalytic reaction, the results nevertheless support the involvement of many of the key proposed organometallic intermediates.



**Scheme 3:** (a) Potential pathways for alkene isomerization and catalytic reactions using different D-labeled substrates. (b) Plausible catalytic cycles under *E*- and *Z*-selective conditions. *Z*-to-*E* isomerization of *Z*-product under *E*-selective conditions (right side). (c) Synthesis, characterization, and reactivity of model  $\pi$ -allyltungsten(II)

complex **W-2**. Under vacuum, **W-2** was converted to dimeric species **W-3** (bottom left). In the 3D structure of **W-3**, the *N*-phenyl groups and all H atoms are removed for clarity (CCDC 2224919). <sup>a</sup> CHCl<sub>3</sub> instead of CDCl<sub>3</sub> for *E*-selective conditions.

Plausible catalytic cycles consistent with the above data are depicted in Schemes 3d and 3e for *Z*- and *E*-selective conditions, respectively. To rationalize the observed intermolecular D-exchange under *E*-selective conditions, a potential pathway arises from a bis alkene complex that undergoes allylic C–H oxidative addition with one alkene, and insertion of the hydride into the other alkene to afford W(II)( $\pi$ -allyl)(alkyl) species. The intermolecular H/D transfer may occur in a concerted or step-wise fashion. Lastly, to support thermodynamic scrambling to the of *Z*- to *E*-product we subjected pure *Z*-alkene (**2a**) to the *E*-selective conditions and observed identical selectivity as the catalytic reaction (**3a**; *E/Z* 3.4:1), establishing that **2a** is a competent intermediate en route to **3a** (Scheme 3c).<sup>62</sup>

## Conclusion

Control of molecular geometry and the use of high coordination number organometallic intermediates has been an overlooked tactic in organic synthesis for achieving stereoselective reactions. This work demonstrates how the stereoselectivity of kinetic alkene isomerization can be affected by different ligand environments, highlighting the sensitivity of the congested 7-coordinate intermediates. We anticipate this method will be useful, particularly when paired with stereoretentive cross-metathesis to form a variety of internal alkenes in which high chemoselectivity is needed.

## Methods

### Supplemental experimental procedure B (E conditions)

An oven-dried 8-mL screw-cap reaction vial containing a Teflon®-coated magnetic stir bar was charged with the alkenyl amide, ketone, or ester **1** (0.10 mmol). The vial was introduced into an argon-filled glovebox, where it was further charged with W(MeCN)<sub>3</sub>(CO)<sub>3</sub> (1.9 mg, 5 mol%) in CDCl<sub>3</sub> (1.0 mL). The tube was sealed then removed from the glovebox and stirred (approximately 800 rpm) at 75 °C for 1 h. After this period of time, the reaction mixture was directly assayed by <sup>1</sup>H NMR. The crude material was purified by flash column chromatography on silica gel with a mixture of hexane/EtOAc as eluent.

### Supplemental experimental procedure C (Z conditions)

An oven-dried 8-mL screw-cap reaction vial containing a Teflon®-coated magnetic stir bar was introduced into an argon-filled glovebox, where it was charged with W(MeCN)<sub>3</sub>(CO)<sub>3</sub> (1.9 mg, 5 mol%) and NHC-**1**•CO<sub>2</sub> (1.4 mg, 10 mol%) in THF (1.0 mL). The solution was stirred at room temperature for 5 min, at which point alkenyl amide, ketone, or ester **1** (0.10 mmol) was added. The tube was removed from the glovebox, and the reaction mixture was stirred (approximately 800 rpm) at 75 °C for 2 h. After this period of time, the reaction mixture was filtered through Celite, and the bed of Celite was washed with acetone. The filtrate was concentrated, and the crude material was purified by flash column chromatography on silica gel with a mixture of hexane/EtOAc as eluent.

## Supporting Information

Details about the materials and methods, experimental procedures, mechanistic studies, characterization data and NMR spectra are available in the Supplementary Information. Accession Codes CCDC 2144251, 2224919 contain the supplementary crystallographic data for this paper. These data can be obtained free of charge via [www.ccdc.cam.ac.uk/data\\_request/cif](http://www.ccdc.cam.ac.uk/data_request/cif), or by emailing [data\\_request@ccdc.cam.ac.uk](mailto:data_request@ccdc.cam.ac.uk), or by contacting The Cambridge Crystallographic Data Centre, 12 Union Road, Cambridge CB2 1EZ, UK; fax: +44 1223 336033. Additional data are available from the corresponding author upon reasonable request.

## AUTHOR INFORMATION

### Author contributions

T.C.J., C.Z.R., H.C.H., and R.M. performed the experimental work and data analysis. T.C.J. and K.M.E wrote the manuscript with input from all authors.

### Correspondence



Correspondence or reasonable requests for material should be addressed to Keary M. Engle, [keary@scripps.edu](mailto:keary@scripps.edu).

## Competing interests

The authors declare no conflicts of interest.

## ACKNOWLEDGMENTS

Financial support for this work was provided by the National Science Foundation (CHE- 2046286). We thank the Schimmel Family Endowed Scholarship Fund for a Graduate Fellowship (C.Z.R.) H.C.H was supported by The Lee Hysan Foundation. R.M.-M. was supported by a La Caixa Predoctoral Fellowship. We thank Materia, Inc. for the donation of metathesis catalysts. Milan Gembicky and Jake Bailey (UCSD) are acknowledged for the collection and analysis of X-ray structures. Jason Chen (Scripps Research) assisted in the separation of *E* and *Z*- isomers for some examples. Skyler D. Mendoza is acknowledged for helpful proofreading of this manuscript. Agnes Trekker is acknowledged for the photo of *Prunus phaesticta* – no rights reserved (cc0).

## REFERENCES

1. Vanderwal, C. D.; Atwood, B. R. Recent Advances in Alkene Metathesis for Natural Product Synthesis—Striking Achievements Resulting from Increased Sophistication in Catalyst Design and Synthesis Strategy. *Aldrichimica Acta* **2017**, *50*, 17–27.
2. Cheng-Sánchez, I.; Sarabia, F. Recent Advances in Total Synthesis via Metathesis Reactions. *Synthesis* **2018**, *50*, 3749–3786.
3. Tomanik, M.; Hsu, I. T.; Herzon, S. B. Fragment Coupling Reactions in Total Synthesis That Form Carbon–Carbon Bonds via Carbanionic or Free Radical Intermediates. *Angew. Chem. Int. Ed.* **2021**, *60*, 1116–1150.
4. Heravi, M. M.; Ghanbarian, M.; Zadsirjan, V.; Alimadadi Jani, B. Recent Advances in the Applications of Wittig Reaction in the Total Synthesis of Natural Products Containing Lactone, Pyrone, and Lactam as a Scaffold. *Monatsh. Chem.* **2019**, *150*, 1365–1407.
5. Donohoe, T. J.; O’Riordan, T. J. C.; Rosa, C. P. Ruthenium-Catalyzed Isomerization of Terminal Olefins: Applications to Synthesis. *Angew. Chem. Int. Ed.* **2009**, *48*, 1014–1017.
6. Armanino, N.; Charpentier, J.; Flachsman, F.; Goetze, A.; Liniger, M.; Kraft, P. What's Hot, What's Not: The Trends of the Past 20 Years in the Chemistry of Odorants. *Angew. Chem. Int. Ed.* **2020**, *59*, 16310–16344.
7. Vasseur, A.; Bruffaerts, J.; Marek, I. Remote Functionalization through Alkene Isomerization. *Nat. Chem.* **2016**, *8*, 209–219.
8. Sommer, H.; Juliá-Hernández, F.; Martín, R.; Marek, I. Walking Metals for Remote Functionalization. *ACS Cent. Sci.* **2018**, *4*, 153–165.
9. Fiorito, D.; Scaringi, S.; Mazet, C. Transition Metal-Catalyzed Alkene Isomerization as an Enabling Technology in Tandem, Sequential and Domino Processes. *Chem. Soc. Rev.* **2021**, *50*, 1391–1406.
10. Crossley, S. W. M.; Obradors, C.; Martínez, R. M.; Shenvi, R. A. Mn, Fe, and Co-Catalyzed Radical Hydrofunctionalizations of Olefins. *Chem. Rev.* **2016**, *116*, 8912–9000.
11. Nicolaou, K. C.; Edmonds, D. J.; Bulger, P. G. Cascade Reactions in Total Synthesis *Angew. Chem. Int. Ed.* **2006**, *45*, 7134–7186.
12. Larsen, C. R.; Grotjahn, D. B. The Value and Application of Transition Metal Catalyzed Alkene Isomerization in Industry. In *Applied Homogeneous Catalysis with Organometallic Compounds*, 3<sup>rd</sup> ed.; Cornils, B.; Herrmann, W. A.; Beller, M.; Paciello, R., Eds.; Wiley-VCH, 2017, pp 1365–1378.
13. Otsuka, S.; Tani, K. Isomerization of Olefin and the Related Reactions. In *Transition Metals for Organic Synthesis: Building Blocks and Fine Chemicals*, 2<sup>nd</sup> ed.; Beller, M., Bolm, C., Eds.; Wiley-VCH, 1998; pp 147–157.
14. Larionov, E.; Li, H.; Mazet, C. Well-Defined Transition Metal Hydrides in Catalytic Isomerizations. *Chem. Commun.* **2014**, *50*, 9816–9826.
15. Liu, X.; Liu, Q. Catalytic Asymmetric Olefin Isomerization: Facile Access to Chiral Carbon-Stereogenic Olefinic Compounds. *Chem Catal.* **2022**, *2*, 2852–2864.
16. Hilt, G. Double Bond Isomerisation and Migration—New Playgrounds for Transition Metal-Catalysis. *ChemCatChem* **2014**, *6*, 2484–2485.
17. Molloy, J. J.; Morack, T.; Gilmour, R. Positional and Geometrical Isomerisation of Alkenes: The Pinnacle of Atom Economy. *Angew. Chem. Int. Ed.* **2019**, *58*, 13654–13664.

18. Yang, W.; Chernyshov, I. Y.; Weber, M.; Pidko, E. A.; Filonenko, G. A. Switching between Hydrogenation and Olefin Transposition Catalysis via Silencing NH Cooperativity in Mn(I) Pincer Complexes *ACS Catal.* **2022**, *12*, 10818–10825.
19. Camp, A. M.; Kita, M. R.; Blackburn, P. T.; Dodge, H. M.; Chen, C.-H.; Miller, A. J. M., Selecting Double Bond Positions with a Single Cation-Responsive Iridium Olefin Isomerization Catalyst. *J. Am. Chem. Soc.* **2021**, *143*, 2792–2800.
20. Liu, X.; Zhang, W.; Wang, Y.; Zhang, Z.-X.; Jiao, L.; Liu, Q. Cobalt-Catalyzed Regioselective Olefin Isomerization Under Kinetic Control. *J. Am. Chem. Soc.* **2018**, *140*, 6873–6882.
21. Wang, Y.; Qin, C.; Jia, X.; Leng, X.; Huang, Z. An Agostic Iridium Pincer Complex as a Highly Efficient and Selective Catalyst for Monoisomerization of 1-Alkenes to *trans*-2-Alkenes. *Angew. Chem., Int. Ed.* **2017**, *56*, 1614–1618.
22. Larsen, C. R.; Erdogan, G.; Grotjahn, D. B. General Catalyst Control of the Monoisomerization of 1-Alkenes to *trans*-2-Alkenes. *J. Am. Chem. Soc.* **2014**, *136*, 1226–1229.
23. Larsen, C. R.; Grotjahn, D. B., Stereoselective Alkene Isomerization over One Position. *J. Am. Chem. Soc.* **2012**, *134*, 10357–10360.
24. Jennerjahn, R.; Jackstell, R.; Piras, I.; Franke, R.; Jiao, H.; Bauer, M.; Beller, M. Benign Catalysis with Iron: Unique Selectivity in Catalytic Isomerization Reactions of Olefins. *ChemSusChem* **2012**, *5*, 734–739.
25. Gauthier, D.; Lindhardt, A. T.; Olsen, E. P. K.; Overgaard, J.; Skrydstrup, T. In Situ Generated Bulky Palladium Hydride Complexes as Catalysts for the Efficient Isomerization of Olefins. Selective Transformation of Terminal Alkenes to 2-Alkenes. *J. Am. Chem. Soc.* **2010**, *132*, 7998–8009.
26. Lim, H. J.; Smith, C. R.; RajanBabu, T. V. Facile Pd(II)- and Ni(II)-Catalyzed Isomerization of Terminal Alkenes into 2-Alkenes. *J. Org. Chem.* **2009**, *74*, 4565–4572.
27. Kobayashi, T.; Yorimitsu, H.; Oshima, K. Cobalt-Catalyzed Isomerization of 1-Alkenes to (*E*)-2-Alkenes with Dimethylphenylsilylmethylmagnesium Chloride and Its Application to the Stereoselective Synthesis of (*E*)-Alkenylsilanes. *Chem. Asian J.* **2009**, *4*, 1078–1083.
28. Hanessian, S.; Giroux, S.; Larsson, A. Efficient Allyl to Propenyl Isomerization in Functionally Diverse Compounds with a Thermally Modified Grubbs Second-Generation Catalyst. *Org. Lett.* **2006**, *8*, 5481–5484.
29. Zhang, S.; Bedi, D.; Cheng, L.; Unruh, D. K.; Li, G.; Findlater, M. Cobalt(II)-Catalyzed Stereoselective Olefin Isomerization: Facile Access to Acyclic Trisubstituted Alkenes. *J. Am. Chem. Soc.* **2020**, *142*, 8910–8917.
30. Yu, X.; Zhao, H.; Li, P.; Koh, M. J. Iron-Catalyzed Tunable and Site-Selective Olefin Transposition *J. Am. Chem. Soc.* **2020**, *142*, 18223–18230.
31. Zhao, J.; Cheng, B.; Chen, C.; Lu, Z. Cobalt-Catalyzed Migrational Isomerization of Styrenes. *Org. Lett.* **2020**, *22*, 837–841.
32. Kapat, A.; Sperger, T.; Guven, S.; Schoenebeck, F., *E*-Olefins through Intramolecular Radical Relocation. *Science* **2019**, *363*, 391–396.
33. Murai, M.; Nishimura, K.; Takai, K. Palladium-Catalyzed Double-Bond Migration of Unsaturated Hydrocarbons Accelerated by Tantalum Chloride. *Chem. Commun.* **2019**, *55*, 2769–2772.
34. Trost, B. M.; Cregg, J. J.; Quach, N. Isomerization of *N*-Allyl Amides to Form Geometrically Defined Di-, Tri-, and Tetrasubstituted Enamides. *J. Am. Chem. Soc.* **2017**, *139*, 5133–5139.
35. Crossley, S. W. M.; Barabé, F.; Shenvi, R. A. Simple, Chemoselective, Catalytic Olefin Isomerization. *J. Am. Chem. Soc.* **2014**, *136*, 16788–16791.
36. Zhuo, L.-G.; Yao, Z.-K.; Yu, Z.-X. Synthesis of *Z*-Alkenes from Rh(I)-Catalyzed Olefin Isomerization of  $\beta,\gamma$ -Unsaturated Ketones. *Org. Lett.* **2013**, *15*, 4634–4637.
37. Mamone, P.; Grünberg, M. F.; Fromm, A.; Khan, B. A.; Gooßen, L. J. [Pd( $\mu$ -Br)(P<sup>t</sup>Bu<sub>3</sub>)<sub>2</sub>] as a Highly Active Isomerization Catalyst: Synthesis of Enol Esters from Allylic Esters. *Org. Lett.* **2012**, *14*, 3716–3719.
38. Mayer, M.; Welther, A.; Jacobi von Wangelin, A. Iron-Catalyzed Isomerizations of Olefins. *ChemCatChem* **2011**, *3*, 1567–1571.
39. Grotjahn, D. B.; Larsen, C. R.; Gustafson, J. L.; Nair, R.; Sharma, A. Extensive Isomerization of Alkenes Using a Bifunctional Catalyst: An Alkene Zipper. *J. Am. Chem. Soc.* **2007**, *129*, 9592–9593.
40. Kim, D.; Pillon, G.; DiPrimio, D. J.; Holland, P. L. Highly *Z*-Selective Double Bond Transposition in Simple Alkenes and Allylarenes through a Spin-Accelerated Allyl Mechanism. *J. Am. Chem. Soc.* **2021**, *143*, 3070–3074.
41. Becica, J.; Glaze, O. D.; Wozniak, D. I.; Dobereiner, G. E. Selective Isomerization of Terminal Alkenes to (*Z*)-2-Alkenes Catalyzed by an Air-Stable Molybdenum(0) Complex. *Organometallics* **2018**, *37*, 482–490.
42. Schmidt, A.; Nödling, A. R.; Hilt, G. An Alternative Mechanism for the Cobalt-Catalyzed Isomerization of Terminal Alkenes to (*Z*)-2-Alkenes. *Angew. Chem., Int. Ed.* **2015**, *54*, 801–804.

43. Weber, F.; Schmidt, A.; Röse, P.; Fischer, M.; Burghaus, O.; Hilt, G. Double-Bond Isomerization: Highly Reactive Nickel Catalyst Applied in the Synthesis of the Pheromone (9Z,12Z)-Tetradeca-9,12-dienyl Acetate. *Org. Lett.* **2015**, *17*, 2952–2955.
44. Chen, C.; Dugan, T. R.; Brennessel, W. W.; Weix, D. J.; Holland, P. L. Z-Selective Alkene Isomerization by High-Spin Cobalt(II) Complexes. *J. Am. Chem. Soc.* **2014**, *136*, 945–955.
45. Carvalho-Junior, E. J.; Oliveira, C. Nickel-Catalyzed Double Bond Transposition Under Kinetic Control. *ChemRxiv* **2022**, DOI: 10.26434/chemrxiv-2022-w9n02 (accessed 01-11-2023).
46. Rubel, C. Z.; Ravn, A. K.; Yang, S.; Li, Z.-Q.; Engle, K. M.; Vantourout, J. C. Stereodivergent, Kinetically Controlled Isomerization of Terminal Alkenes via Nickel Catalysis. *ChemRxiv* **2022**, DOI: 10.26434/chemrxiv-2022-x8ssk (accessed 01-11-2023).
47. Maercker, A. The Wittig Reaction. In *Organic Reactions*, Vol. 14; John Wiley & Sons, 1965; pp 270–490.
48. Nakashima, Y.; Hirata, G.; Sheppard, T. D.; Nishikata, T. The Mizoroki-Heck Reaction with Internal Olefins: Reactivities and Stereoselectivities. *Asian J. Org. Chem.* **2020**, *9*, 480–491.
49. Gao, S.; Shi, L.; Chang, L.; Wang, B.; Fu, J. Recent Developments in Heck-Type Reaction of Unactivated Alkenes and Alkyl Electrophiles *Synthesis* **2021**, *53*, 861–878.
50. Molander, G. A.; Felix, L. A. Stereoselective Suzuki–Miyaura Cross-Coupling Reactions of Potassium Alkenyltrifluoroborates with Alkenyl Bromides. *J. Org. Chem.* **2005**, *70*, 3950–3956.
51. Barder, T. E.; Walker, S. D.; Martinelli, J. R. Buchwald, S. L. Catalysts for Suzuki–Miyaura Coupling Processes: Scope and Studies of the Effect of Ligand Structure. *J. Am. Chem. Soc.* **2005**, *127*, 4685–4696.
52. Kluwer, A. M.; Elsevier, C. J.; de Vries, J. G. *Handbook of Homogeneous Hydrogenation*; Vol. 1, Wiley-VCH, 2007; pp 375–411
53. Nishimura, S. *Handbook of Heterogeneous Catalytic Hydrogenation for Organic Synthesis*; Wiley-Interscience, 2001; p 148.
54. Gnaim, S.; Bauer, A.; Zhang, H.-J.; Chen, L.; Gannett, C.; Malapit, C. A.; Hill, D. E.; Vogt, D.; Tang, T.; Daley, R. A.; Hao, W.; Zeng, R.; Quertenmont, M.; Beck, W. D.; Kandahari, E.; Vantourout, J. C.; Echeverria, P.-G.; Abruna, H. D.; Blackmond, D. G.; Minter, S. D.; Reisman, S. E.; Sigman, M. S.; Baran, P. S. Cobalt-Electrocatalytic HAT for Functionalization of Unsaturated C–C Bonds *Nature* **2022**, *605*, 687–695.
55. Swamy, K. C. K.; Reddy, A. S.; Sandeep, K.; Kalyani, A. Advances in Chemoselective and/or Stereoselective Semihydrogenation of Alkynes. *Tetrahedron Lett.* **2018**, *59*, 419–429.
56. Heath, R. J.; Rock, C. O. Roles of the FabA and FabZ-Hydroxyacyl-Acyl Carrier Protein Dehydratases in *Escherichia coli* Fatty Acid Biosynthesis. *J. Biol. Chem.* **1996**, *271*, 27795–27801.
57. Dodge, G. J.; Patel, A.; Jaremko, K. L.; McCammon, J. A.; Smith, J. L.; Burkart, M. D.; Structural and Dynamical Rationale for Fatty Acid Unsaturation in *Escherichia coli*. *Proc. Natl. Acad. Sci. U. S. A.* **2019**, *116*, 6775–6783.
58. Scheuerbrandt, G.; Goldfine, H.; Baronowsky, P. E.; Bloch, K. A Novel Mechanism for the Biosynthesis of Unsaturated Fatty Acids. *J. Biol. Chem.* **1961**, *236*, 70–71.
59. Jankins, T. C.; Bell, W. C.; Zhang, Y.; Qin, Z.-Y.; Chen, J. S.; Gembicky, M.; Liu, P.; Engle, K. M., Low-Valent Tungsten Redox Catalysis Enables Controlled Isomerization and Carbonylative Functionalization of Alkenes. *Nat. Chem.* **2022**, *14*, 632–639.
60. Jankins, T. C.; Martin-Montero, R.; Cooper, P.; Martin, R.; Engle, K. M. Low-Valent Tungsten Catalysis Enables Site-Selective Isomerization–Hydroboration of Unactivated Alkenes. *J. Am. Chem. Soc.* **2021**, *143*, 14981–14986.
61. Voutchkova, A. M.; Feliz, M.; Clot, E.; Eisenstein, O.; Crabtree, R. H. Imidazolium Carboxylates as Versatile and Selective N-Heterocyclic Carbene Transfer Agents: Synthesis, Mechanism, and Applications. *J. Am. Chem. Soc.* **2007**, *129*, 12834–12846.
62. Pedley, J. B.; Naylor, R. D.; Kirby, S. P., Prediction of Standard Enthalpies of Formation. In *Thermochemical Data of Organic Compounds*; Springer, 1986; pp 7–51.
63. Schreiber, S L, and Crabtree, G.R. The mechanism of action of cyclosporin A and FK506. *Immunology Today* **13**, 136-42. (1992).
64. Paul, C., Graeber, M., Stuetz, A. Ascomycins: promising agents for the treatment of inflammatory skin diseases, *Expert Opinion on Investigational Drugs*, **9**, 69-77 (2000).
65. Ho, C.-L., I-Chen, E., Su, Y.-C. Composition of the Leaf Oils of *Prunus phaeosticta* var. *phaeosticta* From Taiwan, *Journal of Essential Oil Research*, **21**, 345-347 (2009).
66. Koh, M. J.; Khan, R. K. M.; Torker, S.; Yu, M.; Mikus, M. S.; Hoveyda, A. H. High-Value Alcohols and Higher-Oxidation-State Compounds by Catalytic Z-Selective Cross-Metathesis. *Nature* **517**, 181–186 (2015).

67. Sanford, M. S.; Love, J. A.; Grubbs, R. H. A Versatile Precursor for the Synthesis of New Ruthenium Olefin Metathesis Catalysts. *Organometallics* **20**, 5314–5318 (2001).
68. Ditri, T. B.; Moore, C. E.; Rheingold, A. L.; Figueroa, J. S. Oxidative Decarbonylation of *m*-Terphenyl Isocyanide Complexes of Molybdenum and Tungsten: Precursors to Low-Coordinate Isocyanide Complexes. *Inorg. Chem.* **50**, 10448–10459 (2011).
69. Biswas, S. Mechanistic Understanding of Transition-Metal-Catalyzed Olefin Isomerization: Metal-Hydride Insertion-Elimination vs.  $\pi$ -Allyl Pathways. *Comments Inorg. Chem.* **35**, 300–330 (2015).
70. Szymańska-Buzar, T.; Jaroszewski, M.; Wilgocki, M.; Ziółkowski, J. J. Reactivity of Bis(alkene) Tetracarbonyl Complexes of Tungsten: Evidence for Alkene to  $\pi$ -Allyl Hydride Rearrangement. *J. Mol. Catal. A* **112**, 203–210 (1996).
71. Wrighton, M.; Hammond, G. S.; Gray, H. B., Group VI Metal Carbonyl Photoassisted Isomerization of Olefins. *J. Organometal. Chem.* **70**, 283–301 (1974).
72. Iwamoto, H.; Tsuruta, T.; Ogoshi, S. Development and Mechanistic Studies of (*E*)-Selective Isomerization/Tandem Hydroarylation Reactions of Alkenes with a Nickel(0)/Phosphine Catalyst *ACS Catal.* **11**, 6741–6749 (2021).
73. Ryan, D. E.; Cardin, D. J.; Hartl, F.  $\eta^3$ -Allyl Carbonyl Complexes of Group 6 Metals: Structural Aspects, Isomerism, Dynamic Behaviour and Reactivity. *Coord. Chem. Rev.* **335**, 103–149 (2017).
74. Calhorda, M.J.; Costa, P.J. Structure, Bonding and Reactivity of Seven-Coordinate Allylic Mo(II) and W(II) Complexes *Coord. Chem. Rev.* **344**, 83–100 (2017).
75. Ephritikhine, M.; Green, M. L. H.; MacKenzie, R. E. Some  $\eta^1$  and  $\eta^3$ -Allylic and Metallocyclobutane Derivatives of Molybdenum and Tungsten. *J. Chem. Soc., Chem. Comm.* 619–621 (1976).

## TOC Graphic

